≪Research Paper≫ Journal of the Korean Vacuum Society Vol.17 No.6, November 2008, pp.566~575

A Reliable Field Emission Performance of Double-Walled Carbon Nanotube Field Emitters

S. I. Jung and S. B. Lee

Department of Nanoscale Semiconductor Engineering, Hanyang University, Seoul 133-791

(Received August 28, 2008, Revised October 18, 2008, Accepted November 18, 2008)

We investigated the field emission characteristics from the planar field emitters made of double-walled carbon nanotubes (DWCNTs) synthesized by a catalytic chemical vapor deposition (CCVD) method. Transmission electron microscopy, Thermogravimetric and Raman analysis showed that the carbon materials have a low defect level in their atomic carbon structure, pointing to the synthesis of high-purity DWCNTs. For field emission properties of DWCNTs, the turn-on field of DWCNTs was 1.9 V/μm and the current density was about 74 mA/cm^2 at 8.1 V/μm, which is sufficient for the applications of field emission displays and vacuum microelectronic devices. The DWCNT field emitters also exhibited a uniform field emission pattern and good field emission stability in a diode configuration.

Keywords : Double-walled carbon nanotube, Field emission, Saturation-like behavior, Adsorbate

Ⅰ. INTRODUCTION

Since the first discovery of carbon nanotubes (CNTs) in 1991 [1], considerable progress has been made in the synthesis and characterization of CNTs [2-13]. Many research groups have also actively developed their potential applications [14-19]. Among the many potential applications, CNTs have been considered as an ideal field emitter material due to their high aspect ratio and strong C-C covalent bonds in graphene layers [14]. Many researchers have investigated the field emission properties of CNTs in order to apply CNTs to various vacuum microelectronic devices such as field emission displays (FEDs), lamps, x-ray sources, and high-resolution electron beam instruments.

CNTs can be classified into three kinds, viz. single-walled CNTs (SWCNTs), double-walled CNTs (DWCNTs), and multi-walled CNTs (MWCNTs), depending on their tubular structure. Of these, the structure, consisting of two coaxial graphene layers, of DWCNTs is intermediate between those of SWCNTs and MWCNTs. Therefore, a study of DWCNTs should allow us to better understand the structures, basic properties, and practical applications of CNTs [20,21]. Compared with SWCNTs and MWCNTs, DWCNTs have outstanding electrical and mechanical properties due to their coaxial structure reflected in their good electrical conductivity and structural stability [20]. Thus, DWCNTs have the potential to be used in numerous applications in diverse areas in the near future because of their unique structure and properties.

* [E-mail] sbl22@hanyang.ac.kr

Recently, DWCNTs are considered as an ideal candidate for CNT field emitters. As DWCNTs consist of two concentric cylindrical graphene layers, the diameter of the DWCNTs is very close to that of the SWCNTs, which makes the field enhancement factor of the DWCNTs similar to that of the SWCNTs. In addition, the two-graphene layers of DWCNTs make the DWCNTs more resistant to oxidation during field emission than SWCNTs that have only one graphene layer. The turn-on voltage of the DWCNTs for electron emission is as low as that of the SWCNTs and their field emission reliability is similar to that of the MWCNTs [22]. This low turn-on voltage of the DWCNTs, combined with their high brightness and high field-emission reliability offers the promise of their potential application in full color flat panel displays having a large area [23].

In this work, we evaluated the field emission properties of the virgin planar DWCNT field emitters deposited on a Ag/SUS304 substrate by using a spray method. We obtained a stable and reproducible current density (J) versus the electric field (E) curve after several voltage sweeps. At this J-E curve, we achieved a current density of about 74 mA/cm^2 at a high electric field of about 8.1 V/μm from our DWCNT field emitters in a diode configuration. Moreover, the DWCNT field emitters also showed a uniform field emission pattern and stable field emission stability.

Ⅱ. EXPERIMENTS

DWCNTs have been successfully synthesized by a catalytic chemical vapor deposition (CCVD) method using n-hexane as the carbon source and Fe-Mo/MgO as the catalyst at 900 °C. The catalyst preparation and synthesis process have been described in detail elsewhere [26]. The as-synthesized DWCNTs were purified by using a two-step purification process for removing impurities such as amorphous carbon and a catalyst and supporting material so that the effect of such impurities on the field emission property of the DWCNTs can be excluded. We conducted a two-step purification process according to the following procedure. First, the as-synthesized DWCNTs were oxidized in a furnace at 400 °C in the ambient air for 1 hour in order to remove the amorphous carbon material on the surface of the DWCNTs. Second, the oxidized DWCNTs were soaked and sonicated in a dilute 10% acetic acid solution at room temperature. The DWCNT suspension was collected on a Teflon filter with a pore size of 0.2 μm and washed with distilled water several times. Finally, we obtained purified DWCNTs.

The morphologies and microscopic structure of the purified DWCNTs were characterized by scanning electron microscopy (SEM) (HITACHI, S-4700) and high-resolution TEM (HRTEM) (JEOL, JEM-3011, 300 kV). The diameter and crystallinity of the purified DWCNTs were evaluated by Raman spectroscopy (HORIBA JOBIN-YVON, HR800-UV) using Ar laser excitation (laser beam wavelength: 514.5 nm) and the purity of the DWCNTs was evaluated by thermogravimetric analysis (TA Instruments, TGA Q-50).

To evaluate the field emission performance of the purified DWCNTs, the entangled DWCNTs were dipped in ethanol solution and dispersed well by a 30 min ultra-sonication treatment. With optimized spraying parameters, the DWCNT suspensions were sprayed on a Ag paste deposited at a little edge grinded SUS304 disk with an area of 0.19625 cm^2 for 10min using a spray gun. The DWCNTs sprayed on the Ag/SUS304 substrate were dried in air, followed by baking at 350 °C for 20 min in a rapid thermal annealing furnace in an Ar atmosphere to maintain good adhesion and ohmic contact between the DWCNTs and the substrate. Then, the DWCNTs were vertically oriented by a mechanical surface modification to activate using an adhesive tape [27]. We performed field emission measurements through a planar diode configuration in a vacuum chamber at a pressure of less than 2×10^{-7} Torr.

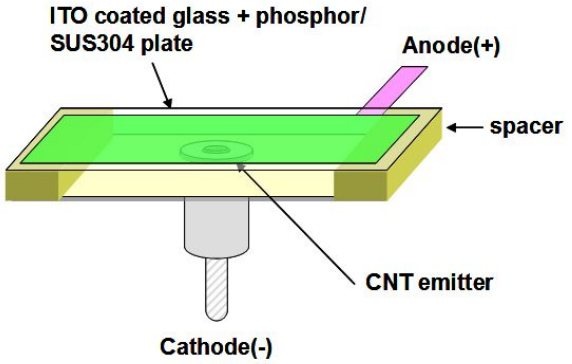

Fig. 1. A schematic diagram of a diode-structured jig with a green phosphor-coated ITO glass used as an anode for measuring emission uniformity or a thick SUS304 plate as the anode for measuring the *J-E* curve, respectively.

The schematic diagram of the jigs used for *J-E* measurements and light emission patterns is illustrated in Fig. 1. The anodes used a SUS304 plate for *J-E* measurements and a green phosphor-coated ITO glass for a light emission pattern, respectively. The gap between the anode and the DWCNT emitters controlled by the thickness of the spacer was 275 μm. Emission current was monitored with a Keithley 6485 and DC power was supplied by a constant power voltage and current controller (HCN140-3500). In this work, we repeated the field emission measurement several times, and the similar *J-E* characteristics were observed.

Ⅲ. RESULTS AND DISCUSSION

Fig. 2(a) is the low resolution SEM image of the purified samples. It shows large amounts of tangled purified carbon filaments, whose lengths are of the order of several tens of micrometers. These filaments

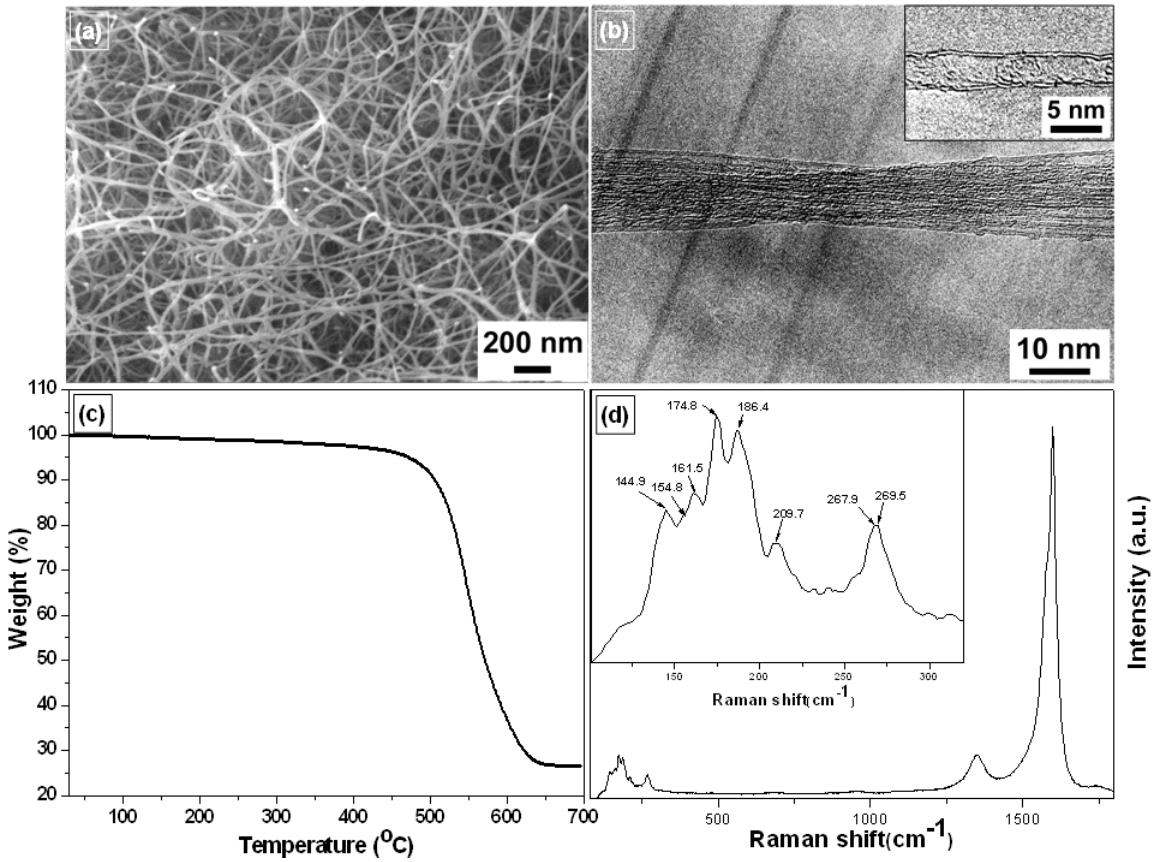

Fig. 2. (a) A SEM image, (b) HRTEM image, (c) TGA data, (d) and Raman spectrum of the purified DWCNTs

seemed to form a layer network and had a clean surface morphology with a high density of bundles. These results revealed that the purified carbon filaments with uniform bundle diameters, ranging from 12 to 29 nm, were produced in fairly high yields.

Fig. 2(b) shows a HRTEM image of the purified carbon filaments. It shows that the purified carbon filaments observed in the SEM image are actually bundles of CNTs consisting of two concentric graphene sheets. As shown in the inset image of Fig. 2(b), isolated DWCNT having an outer diameter of about 3.7 nm was larger than the diameter of individual DWCNT in a bundle. In Fig. 2(b), the purified DWCNTs have clearly resolved graphene layers with no amorphous carbon covering their surface, indicating that they are of high-purity. However, all of the graphene layers showed a wavy structure over a short range revealing the degradation of the graphene layers due to the high acceleration voltage of the electron beam (300 KeV) employed for HRTEM observation. From this HRTEM observation, we observed that the outer and inner diameters of the purified DWCNTs varied in the ranges of 1.5 – 2.7 nm and 0.7 – 1.9 nm, respectively. The diameters of the purified DWCNTs were smaller than those synthesized by arc-discharge.[28-30] In addition, the HRTEM observation indicated that the interlayer spacing of the DWCNTs, ranging from 0.35 – 0.40 nm, was-not a constant. We considered that this increase in the interlayer distance, compared with that of MWCNTs (> 5 layers) having a spacing of 0.34 nm, could result from the high curvature of the DWCNTs due to their small diameter [31].

The purified DWCNTs were thermally analyzed by a thermogravimetric analysis (TGA). The decomposition was conducted in ambient air at a low heating rate of 5 °C/min. As shown in Fig. 2(c), the TGA curve shows that the weight % of the remaining carbon materials became 26 wt% at 654 °C, indicating a carbon yield of about 74 wt%. The residue materials, about 26 %, existed among the purified carbon materials possibly consisting of MgO used as a support material and/or a small amount of Fe-Mo used as a catalyst.

We further performed Raman spectroscopy to characterize the structure and the diameter distribution of the purified DWCNTs. Fig. 2(d) shows a Raman spectrum of the purified samples, clearly indicating the main appearance of the weak D-band at 1329.1 cm^{-1} and the strong G-band at 1572.1 cm^{-1}. The weak D-band revealed that the purified samples consisted of high-purity CNT materials. Generally, the ratio of $I_{(G)} / I_{(D)}$ can be used as an indicator of the extent of disorder within the CNTs. The large value 9.7 of $I_{(G)} / I_{(D)}$ displayed in Fig. 2(d) demonstrated that the defect level in the atomic carbon structure was low, indicating that high-quality DWCNTs were obtained in our experiment. It is known that the radial breathing mode (RBM) can be detected for DWCNTs [32]. Moreover, it was also reported that the same formula could be applied to a SWCNT bundle to calculate the diameter of the DWCNTs within the bundle [33]. In this work, we adopted the expression $\omega = 14 + 224 / d$, where d is a diameter of the DWCNTs and ω is the wavelength of the Raman shift, to calculate the diameter of the DWCNTs, because the purified DWCNTs have bundle shapes [34]. At low Raman shift frequencies, several peaks showed radial breathing modes (RBM), resulting from the different diameters of the CNTs. The RBM peaks at 144.9, 154.8, 161.5, 174.8, 186.4, 209.7, 259.5, 267.9, and 269.4 cm^{-1} of the DWCNTs corresponded to the diameters of 1.711, 1.591, 1.519, 1.393, 1.299, 1.145, 0.912, 0.882, and 0.877 nm, respectively.

From Table 1, concerning the diameter of the purified DWCNTs, we understand that, for a given outer tube diameter, the DWCNTs have different inner tube diameters. This is as a result of the effect of chirality [32]. Generally, nanotubes with a large diameter (> 3 nm) exhibit a weak Raman cross-section. As a result, their band in the low-frequency domain is difficult to detect. However, we deduce that the outer tube diame-

Table 1. Raman peaks and the calculated diameters

The outer tube		The inner tube	
Wavelengh (cm^{-1})	Diameter (nm)	Wavelengh (cm^{-1})	Diameter (nm)
-	2.431	144.9	1.711 nm
-	2.239	161.5	1.519 nm
-	2.019	186.4	1.299 nm
144.9	1.711	259.5	0.912 nm
144.9	1.711	269.4	0.877 nm
154.8	1.591	259.5	0.912 nm
154.8	1.591	269.4	0.877 nm

ters of the purified DWCNTs with inner tube diameters of 1.299, 1.519, and 1.711 nm are about 2.019, 2.239, and 2.431 nm, respectively, as shown in Table 1. This is according to the mean interlayer spacing of the DWCNTs (about 0.36 nm) obtained from the HRTEM observations. With the summarized result from Table 1, the outer diameters of the purified DWCNTs are in the range of 1.591 – 2.431 nm and the inner diameters of the purified DWCNTs are in the range of 0.877 – 1.711nm. The interlayer spacings of the purified DWCNTs range from 0.3395 to 0.4170 nm. We observed that the diameter of the obtained from the Raman analysis was in good agreement with the HRTEM observations.

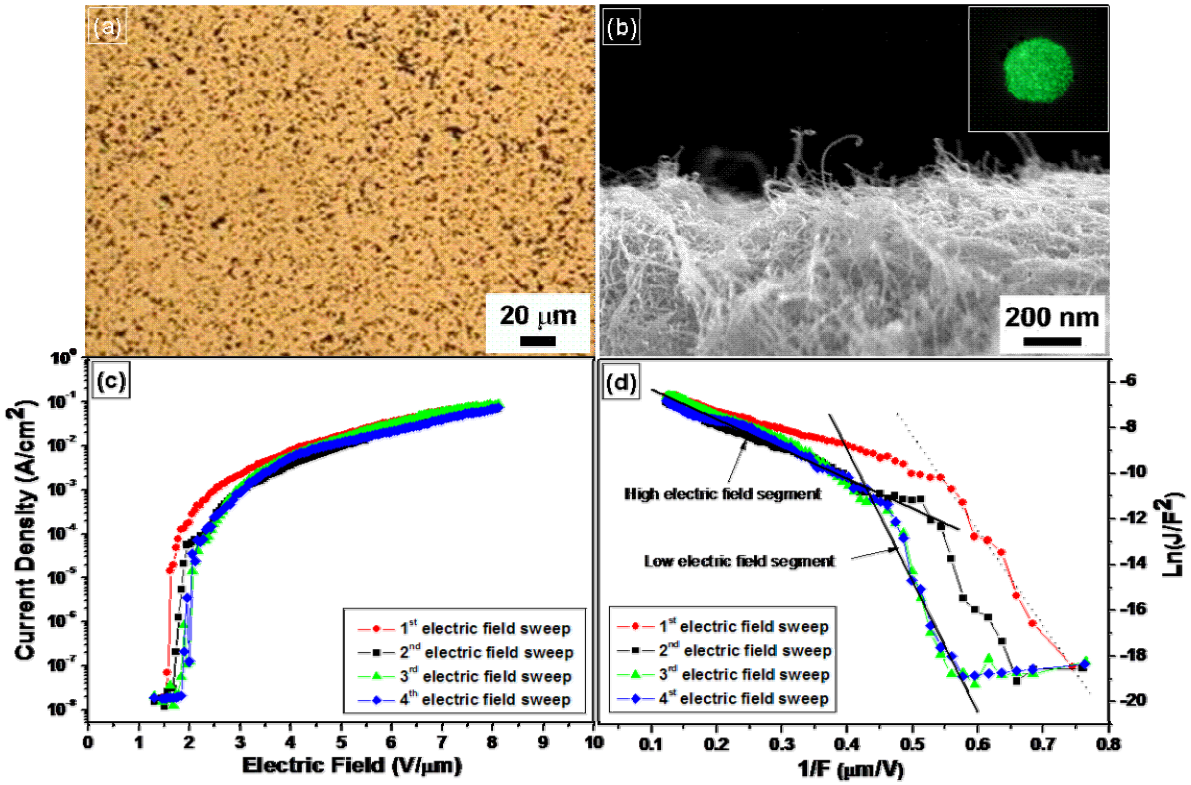

Fig. 3. (a) The optical image of DWCNT field emitters that were strongly deposited on the Ag/SUS304 substrate after mechanical surface modification (b) SEM image of the vertically aligned DWCNTs. The inset is the light emission pattern showing a highly uniform emission. (c) *J*–*E* curves of the DWCNT field emitters sprayed on the Ag/SUS304 substrate. (d) F–N plots corresponding to the *J*–*E* curves of Fig 3(c).

Fig. 3(a) shows an optical image of DWCNT field emitters strongly bound on a Ag/SUS304 substrate after mechanical surface modification. The well-dispersed DWCNT suspensions seemed to be uniformly sprayed on the entire substrate area of 0.19625 cm^2. Consequently, DWCNT field emitters still remained on the Ag/SUS304 substrate in spite of the mechanical surface modification. Fig. 3(b) is a SEM image of the vertically aligned DWCNT field emitters after a treatment of a mechanical surface modification. The emitters showed a very good vertical morphology. By using the measurement configuration in Fig. 1, we observed the field emission pattern so as to identify the emission uniformity of the DWCNT field emitters. As shown in the inset of Fig. 3(b), the DWCNT field emitters sprayed on the Ag/SUS304 substrate revealed a fairly uniform and homogeneous light emission pattern at an electric field of 4 V/μm. It confirmed that our spraying method was very highly efficient allowing avery uniform distribution of DWCNTs.

After confirming a uniform emission pattern, we conducted *J-E* measurements from the jig with a clean SUS304 plate as the anode as shown in Fig. 1. We obtained a stable and reproducible *J-E* curve from the DWCNT field emitters after several electric field sweeps, as shown in Fig. 3(c). The field emission measurements of the DWCNT field emitters were conducted sequentially. The beginning stage of the sequential measurements showed different field emission characteristics. The *J-E* curve in the 1^{st} applied electric field sweep was different from that in the 2^{nd} electric field sweep in the low electric field segment. As the electric field sweep was carried out in a regular sequence, it revealed a stable and reproducible *J-E* curve when drift from the 3^{rd} electric field sweep to the 4^{th} electric field sweep. In other words, the emission current density in the low applied field segment was decreased during the first several electric field sweeps. This kind of decrease of the emission current density in the low electric field segment was quite similar to the result reported by Dean *et al.* [25], where the effect of the adsorbates on the field emission was described. The F-N plots corresponding to *J-E* curves are shown in Fig. 3(d). Firstly, it can be seen that the F-N plot can be divided into two segments: low and high electric field segments. Secondly, it can be seen that the high electric field segment is shrunk and the low electric field segment is shifted to the left as the electric field sweep is repeated. However, after several electric field sweeps, the low electric field segment does not shift to the left any more and we can obtain a reproducible F-N plot. The behavior such as shifting to the left in the F-N plot can be explained by the desorption of adsorbates [24]. Since the DWCNT field emitters were exposed to the air before the field emission measurements, the surface of the emitters must have been covered with adsorbates. These adsorbates can increase the field emission current from the CNT emitters. Conversely, the desorption of these adsorbates can induce a decrease of the field emission current, resulting in this behavior [25]. It is possible that some of the adsorbates released from the surface of the DWCNT field emitters during the first several electric field sweeps can be re-adsorbed on the surface of the DWCNT field emitters during the voltage ramping down. As a result, we needed to make several electric field sweeps to completely desorb the absorbates in our experiment.

A typical turn-on field from the stable *J-E* curve, which produces a current density of 0.1 A/cm^2, is about 1.9 V/μm. It is expected that the turn-on field of the DWCNTs for electron emission may be as low as that of the SWCNTs because of the unique structure of the DWCNTs with small diameters and two graphene layers. In fact, this turn-on field was a little lower than that of arc-SWCNTs [35]. Recently, there have been some reports on the field emission properties of the DWCNTs. The screen-printed DWCNT filmshowed a turn-on field of 1.33 – 1.78 V/μm at an emission current density of 1.0 mA/cm^2 and an emission current density of 0.1–1.7

mA/cm^2 at an applied field of 2.22 V/μm [36]. Kim *et al.* reported that the turn-on field, which produced a current density of 0.1 mA/cm^2, had a field strength of 1.2, 0.95, and 0.9 V/μm, respectively, for DWCNTs grown at 800, 900, and 1000 ºC [37]. Somani *et al.* studied the thick films of DWCNTs deposited on ITO coated glass substrates by a drop casting method and showed a turn-on field of about 0.8 V/μm at a current density of 1 nA/cm^2 and a threshold field of about 1.8 V/μm at a current density of 1 mA/cm^2 [38]. More recently, Ha et. al studied the field emission properties of arc-DWCNTs and obtained a turn-on field of 3.0 V/μm at an emission current density of 0.1 mA/cm^2 [35]. It is difficult to directly compare the field emission performance of each group's results because the field emission properties largely depend on the CNT emitter structure, the CNT species, the CNT morphology, and the field emission measurement techniques. We suggest that our DWCNTs, synthesized by CCVD using n-hexane as a carbon source, exhibited good field emission performances. Moreover, in this work, we achieved a current density of about 74 mA/cm^2 at a high electric field of about 8.1 V/μm from our DWCNT field emittersin a diode configuration.

We also investigated the stability of field emission through the lifetime measurements for the DWCNT field emitters. The initial emission current density was 1.0 mA/cm^2 and then we fixed the applied electric field at 3.1 V/μm for 25 hrs. From Fig. 4, the DWCNT field emitters showed a slight degradation after 25 hrs, indicating a very stable field emission. Compared with the previously reported emission stability of the SWCNTs, the emission stability of the DWCNTs was much better than that of the SWCNTs [30]. We believe that the stable emission properties were caused by two graphene layers and good crystallinity. In fact, the degradation of the CNT tip attached with residual oxygen gases can result in a decrease of emission current density under a high electric field due to Joule heating. The more graphene layers is, the longer the lifetime is. On the other hand, the out-gassing from the electrodes is one of the main reasons for vacuum deterioration, resulting in degradation of emission currents. In this work, deposition of DWCNT films by a spray method is advantageous for high vacuum levels, since there is no organic vehicle as an out gassing source, compared to a conventional screen printing method.

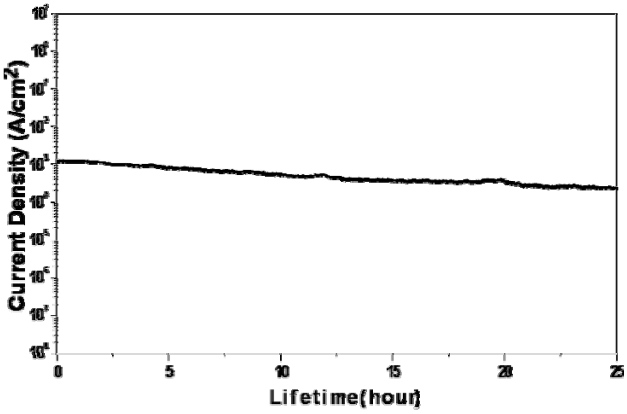

Fig. 4. The lifetime characteristic of the DWCNT field emitters at a constant DC bias corresponding to a current density of 1.0 mA/cm^2

Ⅳ. CONCLUSION

We investigated the field emission characteristics of DWCNT field emitters sprayed on Ag/SUS304 substrates. We obtained a stable and reproducible *J-E* curve after several voltage sweeps. At this *J-E* curve, we achieved a current density of about 74 mA/cm^2 at a high electric field of about 8.1 V/μm from our DWCNT field emitters in a diode configuration. Moreover, The DWCNT field emitters also showed a uniform field emission pattern and stable field emission stability. Therefore, we assert that the DWCNT field emitters can be used as stable field emitters for various field emission applications such as field emission displays, flat lamps, X-ray sources, and electron beam sources.

ACKNOWLEDGEMENT

This work was supported by the Seoul Fellowship. Also, this work was supported by HY-SDR Research Center at Hanyang University and under the ITRC program of Ministry of Knowledge Economy.

참고문헌

[1] S. Iijima, Nature. **354**, 56 (1991).

[2] C. Journet, W. K. Maser, P. Bernier, A. Loiseau, M. Lamy de la Chapelle, S. Lefrant, P. Deniard, R. Lee, J. E. Fischer, Nature. **388**, 756 (1997).

[3] T. Guo, P. Nikolaev, A. Thess, D. T. Colbert, R. E. Smalley, Chem. Phys. Lett. **243**, 49 (1995).

[4] W. Z. Li, S. S. Xie, L. X. Qian, B. H. Chang, B. S. Zou, W. Y. Zhou, R. A. Zhao, G. Wang, Science. **274**, 1701(1996).

[5] M. Terrones, N. Grobert, J. Olivares, J. P. Zhang, H. Terrones, K. Kordatos, W. K. Hsu, J. P. Hare, P. D. Townsend, K. Prassides, A. K. Cheetham, H. W. Kroto, D. R. M. Walton, Nature. **388**, 52 (1997).

[6] A. M. Rao, E. Richter, S. Bandow, B. Chase, P. C. Eklund, K. A. Williams, S. Fang, K. R. Subbaswamy, M. Menon, A. Thess, R. E. Smalley, G. Dresselhaus, M. S. Dresselhaus, Science. **275**, 187 (1997).

[7] R. Sen, A. Govindaraj, C. N. R. Rao, Chem. Phys. Lett. **267**, 276 (1997).

[8] Z. F. Ren, Z. P. Huang, J. W. Xu, J. H. Wang, P. Bush, M. P. Siegal, P. N. Provencio, Science. **282**, 1105 (1998).

[9] J. F. Colomer, G. Bister, I. Willems, Z. Konya, A. Fonseca, G. Van Tendeloo, J. B. Nagy, Chem. Commun. 1343 (1999).

[10] C. L. Cheung, A. Kurtz, H. Park, C. M. Lieber, J. Phys. Chem. B. **106**, 2429 (2002).

[11] L. An, J. M. Owens, L. E. McNeil, J. Liu, J. Am. Chem. Soc. **124**, 13688 (2002).

[12] H. W. Zhu, C. L. Xu, D. H. Wu, B. Q. Wei, R. Vajtai, P. M. Ajayan, Science. **296**, 884 (2002).

[13] W. E. Alvarez, F. Pompeo, J. E. Harrera, L. Balzano, D. E. Resasco, Chem. Mater. **14**, 1853 (2002).

[14] W. A. de Heer, A. Chatelain, D. Ugarte, Science. **270**, 1179 (1995).

[15] P. M. Ajayan, O. Stephan, Ph. Redlich, C. Colliex, Nature. **375**, 564 (1995).

[16] S. J. Tans, M. H. Devoret, H. Dai, A. Thess, R. E. Smalley, L. J. Greeligs, C. Dekker, Nature. **386**, 474 (1997).

[17] G. Che, B. B. Lakshmi, E. R. Fisher, C. R. Martin, Nature. **393**, 346 (1998).

[18] K. H. An, W. S. Kim, Y. S. Park, Y. C. Choi, S. M. Lee, D. C. Chung, D. J. Bae, S. C. Lim, Y. H. Lee, Adv. Mater. **13**, 497 (2001).

[19] K. S. Kim, J. H. Ryu, C. S. Lee, H. E. Lim, J. S. Ahn, J. Jang and K. C. Park, J. Korean Vac. Soc. **17**, 90 (2008).

[20] M. Endo, H. Muramatsu, T. Hayashi, Y. A. Kim, M. Terrones, M. S. Dresselhaust, Nature. **433**, 476 (2005).

[21] R. Saito, R. Matsuo, T. Kimura, G. Dresselhaus, M. S. Dresselhaus, Chem. Phys. Lett. **348**, 187 (2001).

[22] H. Kurachi, S. Uemura, J. Yotani, T. Nagasako, H.Yamada, T. Ezaki, T. Maesoba, R. Loutfy, A. Moravsky, T. Nakagawa, S. Katagiri, Y. Saito, Proceedings of 21st International Display Research Conference/ 8th International Display Workshops: Society for Information Display: San Jose, CA, 2001, pp 1245-1248.

[23] W. B. Choi, D. S. Chung, J. H. Kang, H. Y. Kim, Y. W. Jin, I. T. Han, Y. H. Lee, J. E. Jung, N. S. Lee, G. S. Park, J. M. Kim, Appl. Phys. Lett. **75**, 3129 (1999).

[24] M. Sveningsson, M. Jönsson, O. A. Nerushev, F. Rohmund, and E. E. B. Campbell, Appl. Phys. Lett. **81**, 1095 (2002).

[25] K. A. Dean and B. R. Chalamala, Appl. Phys. Lett.

76, 375 (2000)

[26] S. C. Lyu, B. C. Liu, S. H. Lee, C. Y. Park, H. K. Kang, C. W. Yang, C. J. Lee, J. Phys. Chem. B. **108**, 2192 (2004).

[27] T. J. Vink, M. Gillies, J. C. Kriege and H. W. J. J. Van de Laar, Appl. Phys. Lett. **83**, 3552 (2003).

[28] J. L. Hutchison, N. A. Kiselev, E. P. Krinichnaya, A. V. Krestinin, R. O. Loutfy, A. P. Morawsky, V. E. Muradyan, E. D. Obraztsova, J. Sloan, S. V. Terekhov and D. N. Zakharov, Carbon. **39**, 761 (2001).

[29] Y. Saito, T. Nakahira, S. Uemura, J. Phys. Chem. B. **107**, 931 (2003).

[30] B. Ha, D. H. Shin, J. Park and C. J. Lee, J. phys. Chem. C. **112**, 430 (2008).

[31] C. H. Kiang, M. Endo, P. M. Ajayan, G. Dresselhaus, M. S. Dresselhaus, Phys. Rev. Lett. **81**, 1869 (1998).

[32] S. Bandow, M. Takizawa, K. Hirahara, M. Yudasaka, S. Iijima, Chem. Phys. Lett. **337**, 48 (2001).

[33] W. Ren, F. Li, J. Chen, S. Bai, H. M. Cheng, Chem. Phys. Lett. **359**, 196 (2002).

[34] A. M. Rao, J. Chen, E. Richter, U. Schlecht, P. C. Eklund, R. C. Haddon, U. D. Venkateswaran, Y.-K. Kwon and D. Tománek, Phys. Rev. Lett. **86**, 3895 (2001).

[35] B. Ha, D. H. Shin, J. Park and C. J. Lee, J. phys. Chem. C. **112**, 430 (2008).

[36] Y. D. Lee, H. J. Lee, J. H. Han, J. E. Yoo, Y. H. Lee, J. K. Kirn, S. Nahm, B. K. Ju, J. Phys. Chem. B. **110**, 5310 (2006).

[37] S. Y. Kim, J. Y. Lee, J. Park, C. J. Park, C. J. Lee, H. J. Shin, Chem. Phys. Lett. **420**, 271 (2006).

[38] P. R. Somani, S. P. Somani, S. P. Lau, E. Flahaut, M. Tanemura, M. Umeno, Solid-State Electron. **51**, 788 (2007).

≪연구논문≫ 한국진공학회지 제17권 6호, 2008년 11월, pp.566~575

이중층 탄소나노튜브 전계전자 방출원의 신뢰성 있는 전계방출 특성

정승일 · 이승백

한양대학교 나노반도체공학과, 서울 133-791

(2008년 8월 28일 받음, 2008년 10월 18일 수정, 2008년 11월 18일 확정)

촉매 화학기상증착법을 이용하여 합성된 이중층 탄소나노튜브를 가지고 전계전자 방출원을 제작하여 이들의 신뢰성 있는 전계전자 방출특성을 조사하였다. 합성된 탄소 필라멘트들은 TEM, TGA, 그리고 Raman 분석을 통하여 결함이 없고 순도가 높은 이중층 탄소나노튜브가 합성이 되었음을 확인하였다. 이들 이중층 탄소나노튜브 전계전자 방출원은 이전극 구조에서 낮은 턴-온 전계와 높은 전류밀도의 전계전자 방출 특성을 보여주었고, 균질한 전계방출 패턴과 좋은 전계방출 안정성을 나타내었다.

주제어 : 이중층 탄소나노튜브, 전계 방출, 포화 작용, 흡착물

* [전자우편] sbl22@hanyang.ac.kr